

Comparative Numerical Analysis of Photonic Integrated Tunable Optoelectronic Oscillators Employing High-Q Optical Cavities

Muhammad Imran, Gaurav Pandey,
Claudio Porzi
TeCIP Institute
Scuola Superiore Sant'Anna
Pisa, Italy
muhammad.imran@santannapisa.it

Antonio Malacarne, Paolo Ghelfi
National Lab of Photonic Networks &
Technologies
CNIT
Pisa, Italy

Prof. Antonella Bogoni
TeCIP Institute
Scuola Superiore Sant'Anna
Pisa, Italy
antonella.bogoni@santannapisa.it

Abstract— The performance of two hybrid integrated widely tunable optoelectronic oscillator schemes employing low loss Si_3N_4 microring resonators are compared through computer aided numerical simulation analyses. Optimal device, cavity parameters, and operating conditions leading to enhanced phase noise performance are investigated.

Keywords—Microwave Photonic, Modelling OEO, Photonic

I. INTRODUCTION

Optoelectronic oscillators (OEO) have been widely investigated demonstrating ultra-low phase noise (PN) for microwave (MW) frequency generation, compared to electronic counterparts. Conventional single frequency OEOs typically exploit low-loss optical fiber as an energy storage element to realize a high Q-factor cavity, i.e. exhibiting ultra-low PN, and make use of narrow electrical filter for single mode selection. However, longer cavities imply narrower free spectral range (FSR) resulting in a trade-off between high Q and condition of single mode selection for single-frequency OEO output [1]. Frequency tunability is another desired feature for several applications such as instrumentation, adaptive radars, communication transceivers, phase locked loops [2]. Despite the excellent PN performance, fiber-based OEOs have large size, spurious modes in phase noise spectrum, low stability and restrict tunability because narrow tunable electrical filters are hard to realize at high frequencies. Multiloop OEO architectures and optical and microwave photonic filters (MPF) have been proposed to overcome some of these issues. Alternatively, high-Q integrated optical cavities such as Fabry-Pérot resonators, whispering gallery-mode resonators (WGMR) or micro-ring resonators (MRRs) can also be used as an energy storage element for optical frequency selection [3]. A high-Q resonator acts as a filter to remove the unwanted modes and/or as a modulator in the OEO loop. The bandwidth values associated with high Q factors (e.g., 3×10^5 to 3×10^{11}) are narrow enough to suppress the unwanted modes. Since the Q factor of an OEO is related to the Q factor of its optoelectronic components, the high-Q property of an embedded resonator enhances the OEO PN performance. Furthermore, photonic integrated solutions can significantly reduce the size and improve the stability of OEOs. Recently, several works on full/partially integrated OEOs employing MRR as band-pass [3] and notch filter have been reported [4]. However, the performance is not comparable to the fiber counterparts implying that there is a need for a further investigation of behavior of integrated OEOs including practical constraints and considerations of integration platforms. In this work, we evaluate two schemes for integrated tunable OEOs, and analyze the expected

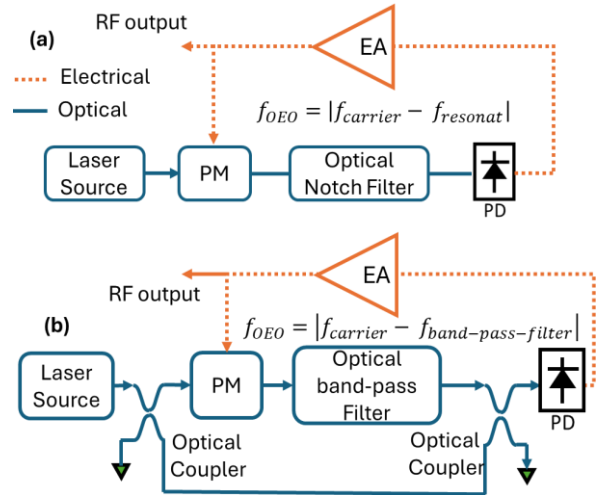


Figure 1 Reference architectures: tunable integrated OEO architectures employing MRR based optical notch filter (a) and bandpass filter (b).

behavior through numerical simulations considering realistic device parameters and platform performance.

II. REFERENCE INTEGRATED OEO ARCHITECTURES

The reference architectures considered for comparative analysis are shown in Fig. 1. The differentiating factor between the two is the method of realizing the MW photonic filter function. In both cases a phase modulated signal is generated by modulating the input optical carrier, $f_{carrier}$, through an optoelectronic phase modulator (PM). The first architecture exploits the notch filter response MRR to perform phase-to-amplitude modulation conversion through sideband suppression and phase rotation at resonant frequency. In the second architecture, a sideband from the PM output is selected through an optical band-pass filter realized by an MRR which is then coupled with the laser optical carrier and fed to a photodetector (PD). The spacing between input optical carrier frequency and filter resonant frequency ($f_{resonant}$ or $f_{band-pass-filter}$) determines the central frequency of the MPF and the OEO output frequency, f_{OEO} . The f_{OEO} can be tuned by either tuning the $f_{carrier}$ or $f_{resonant}$ (for arch.1) or $f_{band-pass-filter}$ (for arch. 2).

III. NUMERICAL ANALYSIS : ASSUMPTIONS & RESULTS

In this study, we opted for computer aided numerical simulations using VPI Photonics™ instead of using analytical models [5]. These tools have several advantages such as repository of electronic & photonics device models, frequency and time domain simulations and analysis, and co-simulation.

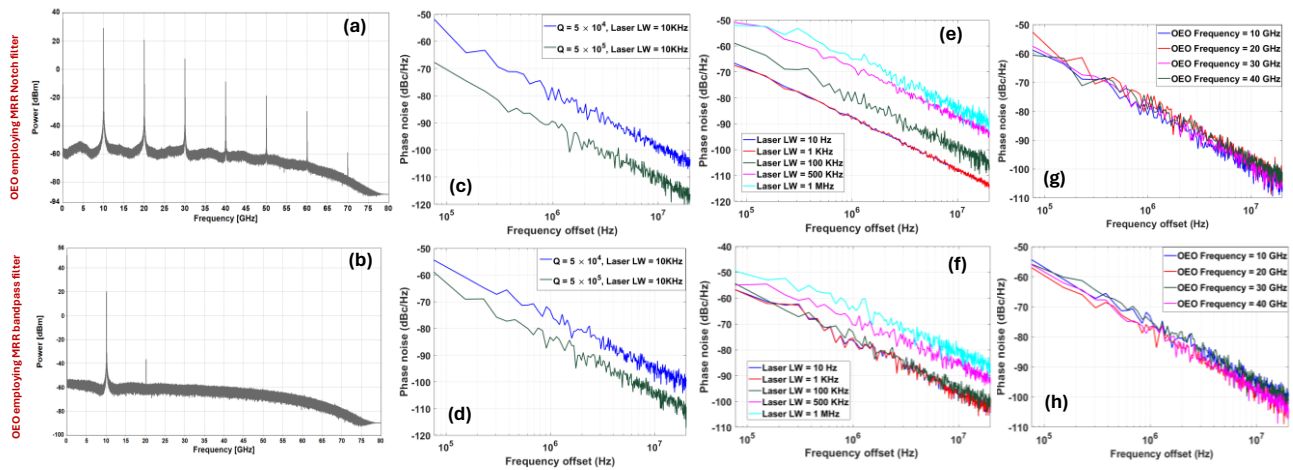


Figure 2 Simulation Results: Comparative performance analysis of two tunable integrated OEO architectures (a & b) OEO output spectra (c-h) Impact on PN performance (c, d) of MRR filter Q-factor (e, f) laser linewidth (LW) (g, h) frequency tunability, (RBW = 76 kHz)

A. Simulator description and assumptions

Both the OEO schemes employing an MRR filter in all-pass (notch) and add-drop (band pass) configurations respectively, were implemented in the simulator. Since an OEO is a feedback architecture, the simulator was set to operate in time domain to understand the evolution of signal within OEO cavity. Appropriate number of samples N_{sam} and sample rate were chosen such that the simulation bandwidth (time window) is sufficiently broader than filter bandwidth to achieve a sufficient frequency resolution. A set of N_{sam} samples go through multiple iterations in OEO cavity until the steady state is achieved for the desired oscillation frequency. The status of signal was monitored and recorded at different stages in the scheme e.g., PM output, MRR output etc., for each iteration. The final temporal output waveform was exported to a MATLAB script to compute PN estimation. The drawback of VPI-based simulations is that the numerical simulations become computationally intensive (and time consuming) as we increase the N_{sam} to achieve the finer frequency resolutions required for PN estimation. Although we understand that PN value for offset frequencies lower than 100 kHz is relevant, however, due to limited computational resources, the frequency resolution for the reported analyses is limited to 76kHz, as it is sufficient to understand the trend of PN performance. Simulations for different photonic integrated technologies/platforms can be run in the simulator and corresponding parameters such as propagation loss, effective index n_{eff} and group index n_g etc., can be incorporated. In both schemes, we consider an MRR on silicon nitride (Si_3N_4) (WG loss = 50 dB/m, $n_{eff} = 1.53$, $n_g = 1.767$) platform whereas power couplers/splitters, PM and PD are assumed in silicon on insulator (SOI). A 40-GHz PM and a 50-GHz PD optoelectronic bandwidth were considered. The electrical amplifier has 50 GHz bandwidth. The two 1 cm electrical delays consider physical length of connections. Propagation loss and delay for each component was included.

B. Results

We characterized the MRR based filters for different high-Q values and analyzed the performance of OEOs in terms of tunability and PN by varying the device parameters (e.g., laser power, RIN, linewidth) and operating conditions. Fig. 2 depicts the performance results of both architectures under similar conditions. In the RF spectrum of OEO output (Fig. 2 (a & b)), harmonics can be clearly observed in both cases,

although less significant for band-pass case because only one sideband mode from phase modulated signal is selected by the band-pass filter and combined with optical carrier. For single frequency OEO operation harmonics would need to be filtered out. The harmonic level can be further reduced by reducing the nonlinearities. Fig. 2(c & d) show the impact of MRR Q-factor on the PN performance of OEO. Reduction in PN with increase in Q factor can be clearly observed in both cases. As evident from Fig. 2 (e & f) the PN of an OEO is significantly affected by the laser LW. Larger LW adds more PN from optical carrier. The PN performances for LW < 100 kHz are same because of resolution bandwidth limitation as explained earlier. OEO tunability (10 – 40 GHz) is demonstrated (Fig. 2 (g & h)), in both cases, PN performance is nearly independent of f_{OEO} , as expected for an OEO operation. The maximum achievable OEO frequency is only limited by the bandwidth of the components in the loop. From the analyses we can conclude that OEOs employing high Q MRR as band pass filter have less harmonics and are suitable for single frequency operation whereas the PN performance of both schemes is similar. In terms of tunability, both schemes are comparable. The optimal setting of device parameters and operating conditions are essential to achieve ultralow PN in addition to increasing the Q-factor.

ACKNOWLEDGMENT

The work was supported Air Force European Office of Aerospace Research and Development under award number FA8655-22-1-7073 and in part by PON ‘‘Ricerca-Innovazione’’ 2014-2020 MUR, Italy.

REFERENCES

- [1] L. Maleki, ‘The opto-electronic oscillator (OEO): Review and recent progress’, in 2012 European Frequency and Time Forum, pp. 497–500.
- [2] M. Li, T. Hao, W. Li, and Y. Dai, ‘Tutorial on optoelectronic oscillators’, APL Photonics, vol. 6, no. 6, p. 061101, Jun. 2021.
- [3] P. T. Do, C. Alonso-Ramos, X. Le Roux, I. Ledoux, B. Journet, and E. Cassan, ‘Wideband tunable microwave signal generation in a silicon-micro-ring-based optoelectronic oscillator’, Sci Rep, vol. 10, no. 1, Art. no. 1, Apr. 2020.
- [4] T. Cui et al., ‘Tunable optoelectronic oscillator based on a high-Q microring resonator’, Optics Communications, vol. 536, p. 129299, Jun. 2023, doi: 10.1016/j.optcom.2023.129299
- [5] E. C. Levy, M. Horowitz, and C. R. Menyuk, ‘Modeling optoelectronic oscillators’, J. Opt. Soc. Am. B, JOSAB, vol. 26, no. 1, pp. 148–159, Jan. 2009.